Adiabatic Pumping of Chern-Simons Axion Coupling

Maryam Taherinejad* and David Vanderbilt
Department of Physics and Astronomy, Rutgers University, Piscataway, New Jersey 08854-0849, USA
(Dated: November 10, 2014)

We study the adiabatic pumping of the Chern-Simons axion (CSA) coupling along a parametric loop characterized by a non-zero second Chern number $C^{(2)}$ from the viewpoint of the hybrid Wannier representation, in which the Wannier charge centers (WCCs) are visualized as sheets defined over a projected 2D Brillouin zone. We derive a new formula for the CSA coupling, expressing it as an integral involving Berry curvatures and potentials defined on the WCC sheets. We show that a loop characterized by a non-zero $C^{(2)}$ requires a series of sheet-touching events at which 2π quanta of Berry curvature are passed from sheet to sheet, in such a way that e^2/h units of CSA coupling are pumped by a lattice vector by the end of the cycle. We illustrate these behaviors via explicit calculations on a model tight-binding Hamiltonian and discuss their implications.

PACS numbers: 03.65.Vf,73.20.At,73.43.-f,71.15.Rf,75.85.+t

The response of materials to electromagnetic fields has been the subject of studies for many years, both for reasons of fundamental interest and for technological applications. The discovery of topological insulators (TIs) and related classes of materials in recent years has generated interest in the Chern-Simons axion (CSA) coupling, which makes an isotropic contribution α^{CS} to the magnetoelectric response tensor of the material. This coupling is conventionally expressed in terms of a dimensionless parameter θ defined via

$$\alpha_{ij}^{\mathrm{CS}} = \frac{\theta e^2}{2\pi h}\delta_{ij}, \tag{1}$$

where θ is determined by the band structure of the insulator via an integral over the Brillouin zone (BZ) of a Chern-Simons 3-form according to

$$\theta = -\frac{1}{4\pi}\int d^3k\,\epsilon^{ijk}\,\mathrm{Tr}[A_i\partial_j A_k - i\frac{2}{3}A_iA_jA_k]. \tag{2}$$

Here $A_i^{nm} = i\langle u_n|\partial_i|u_m\rangle$ is the Berry connection (or non-Abelian gauge field) in Cartesian direction i, where $u_n(\mathbf{k})$ is the periodic part of the Bloch function of the n'th occupied band, and the trace is over occupied bands.

The ground-state properties of a band insulator are invariant under any gauge transformation, that is, any unitary transformation $U_{nn'}(\mathbf{k})$ that mixes only the occupied bands. It can be shown that an arbitrary gauge transformation either leaves the 3-form integral in Eq. (2) unchanged or else shifts it by exactly 2π times an integer. Thus, θ is best regarded as a phase angle that is only well-defined modulo 2π. As a consequence, the presence of either time reversal (TR) or inversion (either of which flips the sign of θ) requires θ to be quantized to an integer multiple of π, with an odd/even value corresponding to an odd/even strong Z_2 topological index of a TR-invariant 3D insulator.[1,2] One way to understand the ambiguity of θ modulo 2π, which corresponds to an ambiguity of α^{CS} modulo e^2/h, is to realize that the magnetoelectric coupling is related to the surface anomalous Hall conductivity (AHC) by $\sigma = (\theta/2\pi + C)e^2/h$. Thus while θ can be calculated from the bulk band structure, the measurable magnetoelectric response can be changed by a quantum if a layer with non-zero Chern number is attached to the surface of material, changing the effective value of θ by 2π.

An interesting consequence of this 2π ambiguity is that if an insulator is allowed to evolve adiabatically around a closed loop in the space of parameters determining the crystal Hamiltonian, with the gap remaining open, then the fact that the system returns to the initial physical state means that θ must either return to its original value or change by an integer multiple of 2π, where the integer $C^{(2)}$ is known as a "second Chern number." This possibility of "pumping θ by 2π" has been discussed and demonstrated for some theoretical models,[1,2] but the characteristic behaviors of a system undergoing such an adiabatic loop have largely remained unexplored.

Recently, we have shown that the hybrid Wannier representation can be a useful and insightful tool for computing topological indices and inspecting the topological properties of 3D insulators.[3] In this approach, the occupied-state wavefunctions are transformed into a maximally-localized Wannier representation in one chosen Cartesian direction, while remaining Bloch-like in the orthogonal directions. The resulting hybrid Wannier functions (HWFs) inherit the topological character of the insulator, and plots of their Wannier charge centers (WCCs) over the 2D BZ ("Wannier sheets") were shown to provide a useful means of visualizing the topological properties of insulators, allowing to discriminate immediately between normal, strong topological, weak topological, crystalline topological, and related states.[3–6]

With these motivations, we ask what happens if an adiabatic cycle that pumps θ by 2π is viewed from the point of view of the HWF representation. How do the WCC sheets evolve? Is there a characteristic behavior of this evolution of the WCC sheets that signals the presence of a non-trivial cycle (i.e., a non-zero second Chern number)? We find that there is indeed such a characteristic behavior. Specifically, we show that quanta e^2/h of Berry curvature are passed from one WCC sheet to the

next in a series of isolated band-touching events, in such a way that one quantum of Berry curvature is pumped by an entire lattice vector by the close of the cycle. We illustrate this amusing and instructive result via numerical calculations on a 3D spinor tight-binding model and discuss its implications.

We begin with a brief review of the construction of the hybrid Wannier representation. We choose a special direction, here $\hat{z}$, along which the Wannier transformation is carried out, so that the HWFs are localized in z while remaining Bloch-like in the other two directions.[7,8] Explicitly,

$$|W_{ln}(k_x,k_y)\rangle = \frac{c}{2\pi}\int dk_z e^{i\mathbf{k}\cdot(\mathbf{r}-lc\hat{z})}|u_{n,\mathbf{k}}\rangle, \qquad (3)$$

where l is a layer index and c is the lattice constant along $\hat{z}$. In general, there is a $U(N)$ gauge freedom in choosing the N representatives of the occupied space, $|\tilde{u}_{n,\mathbf{k}}\rangle = \sum_m U_{nm}|u_{m,\mathbf{k}}\rangle$, but there is a unique gauge that minimizes the spread functional of the WFs along $\hat{z}$.[8] These maximally localized HWFs and their WCCs $\bar{z}_n(k_x,k_y) = \langle W_{n0}|z|W_{n0}\rangle$ can be constructed using standard methods.[8,9]

For a 2D insulator the WCCs can be plotted as curves $\bar{z}_n$ vs. $k_\perp$ in a 1D projected BZ,[4,10] while for a 3D insulator they can be visualized as sheets plotted over the 2D projected BZ. In previous work[3] we have shown that these WCC sheets provide an insightful characterization of the topological character of the insulator in question, allowing one to see how electrons are adiabatically pumped along $\hat{z}$ as k_x and k_y are varied. For example, in a 2D Chern insulator the WCCs shift by one or more lattice constants along z as k_x evolves across the projected BZ, pumping units of charge along that direction. This extra charge is removed from the edge as the edge band crosses the Fermi energy. Time reversal invariant (TRI) insulators have zero Chern numbers but are characterized by Z_2 topological indices that are also reflected in the structure of WCC sheets. For example, a 3D TRI insulator is characterized by one strong and three weak Z_2 indices, which can be determined by examining how the WCC sheets connect along TRI lines in the projected BZ for different Wannierization directions.[3]

It is also of interest to consider the behavior of the WCC sheets as the crystal Hamiltonian is carried adiabatically around a loop defined by some cyclic parameter α corresponding, e.g., to some combination of atomic displacements and/or external fields. A celebrated result of Thouless[11] is that this results in quantized adiabatic charge transport, i.e., the pumping of exactly one electron per unit cell by a lattice vector $\mathbf{R}$ during the cycle. Normally $\mathbf{R}=\mathbf{0}$, but for example if $\mathbf{R}=c\hat{z}$ this corresponds to the pumping of one electron by one period along z during the cycle (a first Chern number of $C=1$), i.e., a change in electric polarization $\Delta P_z = -e/A_{\rm cell}$ with $A_{\rm cell}$ the projected unit cell area.

Let us see how this evolution occurs from the viewpoint of the HWF representation. Intuitively, we expect each WCC sheet to drift along z with increasing α such that it replaces the one above it, and is replaced by the one below it, at the end of the cycle. We begin by defining Berry potentials "living on the sheets" representation as

$$A_{x,ln,l'm} = \langle W_{ln}|i\partial_x|W_{l'm}\rangle\,, \qquad (4)$$

and similarly for A_y. These are functions of (k_x,k_y) and also matrices in the space of sheet labels ln (the $n^{\rm th}$ sheet in cell l along z). The corresponding Berry potentials in the Bloch representation are then just

$$A_{x,nm}(\mathbf{k}) = \sum_l e^{ik_z lc}A_{x,0n,lm}(k_x,k_y)\,, \qquad (5)$$

$$A_{z,nm}(\mathbf{k}) = \bar{z}_n(k_x,k_y)\,\delta_{nm}\,. \qquad (6)$$

Plugging into the Berry-phase formula for the electronic contribution $P_j = -e(2\pi)^{-3}\sum_n\int d^3k\,A_{jn}(\mathbf{k})$, we find

$$P_j = \frac{-e}{(2\pi)^2 c}\sum_n\int d^2k\;A_{j,0n,0n}(k_x,k_y)\,, \qquad (7)$$

$$P_z = \frac{-e}{(2\pi)^2 c}\sum_n\int d^2k\;\bar{z}_n(k_x,k_y)\,, \qquad (8)$$

where $j=\{x,y\}$ in Eq. (7). For the case of a parametric loop that pumps electrons along z, the change $\Delta P_z = -e/A_{\rm cell}$ would occur via the gradual migration of the $\bar{z}(k_x,k_y)$ along the $+\hat{z}$ direction, with a relabeling of sheets required at the end of the loop.

Now we again consider an adiabatic cycle in a 3D insulator, but instead of resulting in the pumping of charge, we examine the case where it results in the pumping of the CSA coupling, increasing θ by $2\pi N$ where N is a nonzero integer (second Chern number $C^{(2)}=N$). This corresponds to a pumping of Berry curvature, instead of electric charge, along z during the adiabatic cycle. For this purpose we now extend the above discussion by defining a Berry curvature on the WCC sheets as $\Omega_{xy,ln,l'm}(k_x,k_y) = i\langle\partial_x W_{ln}|\partial_y W_{l'm}\rangle - i\langle\partial_y W_{ln}|\partial_x W_{l'm}\rangle$. The relation to the Berry curvature in the Bloch representation is similar to that for A in Eq. (5), namely

$$\Omega_{xy,nm}(\mathbf{k}) = \sum_l e^{ik_z lc}\Omega_{xy,0n,lm}(k_x,k_y)\,. \qquad (9)$$

The intrinsic AHC σ_{yx} of the crystal is just given by integrating the trace of Ω_{xy} in the Bloch representation over the 3D BZ, and this is easily shown to be equal to $(e^2/hc)\sum_n C_n$ where C_n is the Chern number of the $n^{\rm th}$ sheet in the home unit cell, given by $C_n = (2\pi)^{-1}\int d^2k\,\Omega_{xy,0n,0n}$. We shall exclude quantum anomalous Hall insulators from our discussion here, so we can assume that $\sum_n C_n = 0$, but importantly the individual C_n can be nonzero.

We now address the central issue of this Letter, namely, how to represent the CSA coupling θ in the HWF representation. Starting from Eq. (2), this can be written as

$$\theta = \theta_{z\Omega} + \theta_{\Delta xy} \qquad (10)$$

where

$$\theta_{z\Omega} = -\frac{1}{2\pi}\int d^3k\,\mathrm{Tr}[A_z\Omega_{xy}]\,, \tag{11}$$

$$\theta_{\Delta xy} = -\frac{1}{2\pi}\int d^3k\,\mathrm{Tr}[A_y\partial_z A_x - iA_z[A_x,A_y]]\,. \tag{12}$$

Performing the k_z integrals with the aid of Eqs. (5), (6) and (9), these are expressed in the HWF representation as

$$\theta_{z\Omega} = -\frac{1}{c}\int d^2k\sum_n \bar{z}_n\,\Omega_{xy,0n,0n}\,, \tag{13}$$

$$\theta_{\Delta xy} = \frac{i}{c}\int d^2k\sum_{lmn}(\bar{z}_{lm}-\bar{z}_{0n})A_{x,0n,lm}A_{y,lm,0n}\,, \tag{14}$$

where $\bar{z}_{lm} = lc + \bar{z}_m$. In deriving Eq. (14) we have used that

$$\frac{c}{2\pi}\int dk_z\mathrm{Tr}[A_y\partial_z A_x] = \sum_l\sum_{nm}(ilc)A_{x,0n,lm}A_{y,lm,0n}\,. \tag{15}$$

Eqs. (10) and (13-14) constitute a major result of the present work. Note that the integrands in Eqs. (13-14) are gauge-invariant in the Bloch directions, i.e., unchanged under a phase twist $\exp(i\varphi_n(k_x,k_y))$.

Of primary concern to us here is the "Berry curvature dipole" term $\theta_{z\Omega}$ in Eq. (13), which describes the extent to which concentrations of positive and negative Berry curvature on the WCC sheets, given by $\Omega_{xy,0n,0n}(k_x,k_y)$, are displaced from one another along the $\hat{z}$ direction as given by $\bar{z}_n(k_x,k_y)$. Note that $\theta_{z\Omega}$ is shifted by $-2\pi C_n$ if the choice of WCC sheets comprising the home unit cell is changed so as to shift some $\bar{z}_n$ by c. The $\theta_{z\Omega}$ term is therefore the one that has the 2π ambiguity, and we shall see that it is responsible for the pumping of CSA coupling in a non-trivial adiabatic cycle. The second term $\theta_{\Delta xy}$, given by Eq. (14), is a kind of intersheet contribution to θ, in which the z-separation between sheets at (k_x,k_y) is coupled to the off-diagonal (inter-sheet) matrix elements of the Berry potentials. There is no 2π ambiguity associated with this term, and as we shall see, it typically remains small even when θ is at or near π. We regard it as a non-topological correction term that is needed for quantitative accuracy but does not otherwise play a role in understanding the topology of an insulator or the evolution of its CSA coupling.

We now illustrate the concepts introduced above in the context of a simple tight-binding model. Following Essin *et al.*,[1] we start with the Fu-Kane-Mele (FKM) model,[12] which is a four-band model of s orbitals on a diamond lattice with spin-orbit interaction,

$$H_{\mathrm{FKM}} = \sum_{<ij>} t(\mathbf{e}_{ij})\,c_i^\dagger c_j + i\lambda_{\mathrm{so}}\sum_{\ll ij\gg} c_i^\dagger \mathbf{s}\cdot(\mathbf{d}_{ij}^1\times\mathbf{d}_{ij}^2)c_j\,. \tag{16}$$

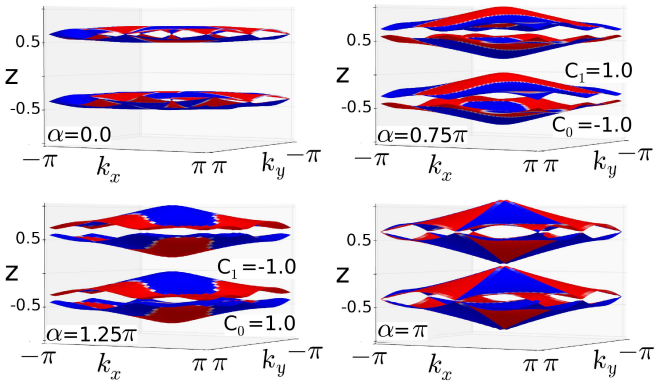

FIG. 1: The two WCC sheets of the half-filled FKM model, and one set of periodic images, at four stages $\alpha = (0,\,3\pi/4,\,\pi,\,5\pi/4)$ along the parametric cycle (clockwise from upper left). Blue and red colors show positive and negative values of Berry curvature Ω_z on the sheets. The Chern numbers associated with the individual WCC sheets are shown for those cases where sheets do not touch.

The first term is a sum over first-neighbor hoppings, where $\mathbf{e}_{ij}$ is the bond vector, while the second term involves second-neighbor hops in which vectors $\mathbf{d}_{ij}^{1,2}$ describe the two first-neighbor bonds that make up the second-neighbor hop. We take the cubic lattice constant to be unity. In the original FKM model $t(\mathbf{e}_{ij}) = t_0$ independent of hopping direction, but following Ref. 1 we take $t(\mathbf{e}_{ij}) = t_0(3+\delta)$ for the bond along (111) and t_0 for the other three bonds. We set the first-neighbor and spin-dependent second-neighbor hoppings to $t_0 = 1$ and $\lambda_{\mathrm{so}} = 1$ respectively, and assume two bands are occupied.

Starting from cubic symmetry at $\delta = -2$, where there are gap closures at the high-symmetry X points, the symmetry is lowered and the gap is opened as δ is varied, allowing trivial, weak, and strong topological phases to be accessed.[3] The strong topological and trivial phases are separated from each other by a band touching at the Γ point when $\delta = 0$. Again following Essin *et al.*[1] we add a staggered Zeeman field h, and define an adiabatic loop parametrized by $\delta(\alpha) = m\cos(\alpha)$ and $h(\alpha) = m\sin(\alpha)$ where α runs from 0 to 2π, such that the system remains insulating on the loop and θ is pumped by 2π. The HWF representation is constructed with $\hat{z}$ along the (111) direction, parallel to the bond with altered hopping strength.

The WCC sheets derived from the two occupied bands in the FKM model are shown in Fig. 1, where one pair of sheets and one copy of their periodic images along $\hat{z}$ are shown for some points around the adiabatic loop. The evolution of the Wannier sheet positions at the four TRI points, namely at Γ and at the three equivalent M points, is plotted in Fig. 2.

The system has TR symmetry at $\alpha = 0$ and π, where the system is Z_2-even and Z_2-odd respectively, and where the WCC sheets pair up at the four TRI-points due to Kramers degeneracy.[3] In the normal phase at $\alpha = 0$ this

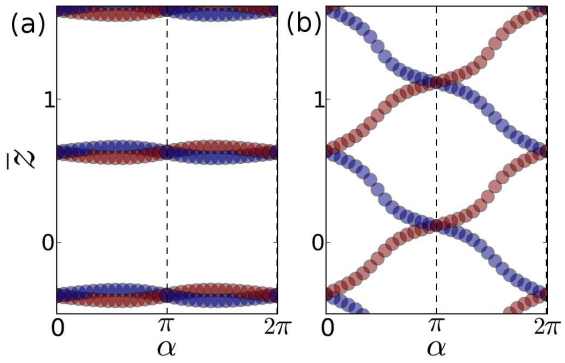

FIG. 2: The WCCs at the (a) M-point and (b) Γ-point as they evolve around the adiabatic loop. Blue and red colors show positive and negative values of Berry curvature at these points.

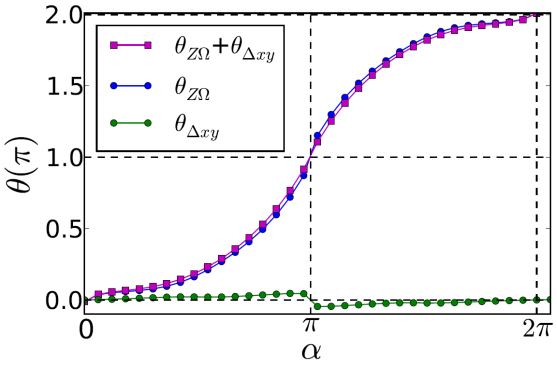

FIG. 3: The CSA coupling $\theta(\alpha)$, and the contributions of the topological term $\theta_{z\Omega}$ and the correction term $\theta_{\Delta xy}$, for the FKM model as it evolves around the adiabatic loop.

results in a pair of sheets connected by Dirac points at all four TRI momenta, and each pair is well separated from its neighbors along $\hat{z}$. As α increases, the Dirac crossings are gapped and the sheets begin to separate. At the three M points the separation between the pair remains quite small, and the same sheets touch again at $\alpha = \pi$, as is obvious from Fig. 2(a). At the Γ point, however, the behavior is much more interesting; the sheets separate strongly and eventually reconnect with their neighbors from the next unit cell along $\hat{z}$ when $\alpha = \pi$. The swapping of partners at an odd number of the TRI points (here, only at Γ) is characteristic of the strong topological (Z_2-odd) phase at $\alpha = \pi$. Note, however, that the WCC sheets, taken together, have no net displacement along the $\hat{z}$ direction, so no charge is pumped.

Now we ask what happens to the CSA coupling θ during this cycle, and to do this we inspect the Berry curvature Ω_{xy} on the sheets. This is represented by the color-scale shading in Figs. 1 and 2. Recall that the evolution of θ is expected to be reflected in the behavior of the $\theta_{x\Omega}$ term as given by Eq. (13). We immediately see that the behavior near the M points is uninteresting; positive and negative Berry curvature contributions separate slightly at first, but they then reverse and recross, and never give a large contribution to $\theta_{z\Omega}$.

Near Γ, however, the story is strikingly different. A negative (red) increment of Berry curvature is transported along $+\hat{z}$ while a positive (blue) contribution is carried along $-\hat{z}$ as α evolves from 0 to π. For small and positive α we intuitively expect that the total Berry curvature near Γ in the top and bottom sheets (at $\bar{z}_2$ and $\bar{z}_1$) should be $-\pi$ and π respectively, characteristic of a weakly gapped Dirac point. Thus the contribution to the Berry curvature dipole term $\theta_{z\Omega}$ from the vicinity of Γ, which is approximately $\pi(\bar{z}_2(0,0) - \bar{z}_1(0,0))/c$, grows gradually as α increases and the sheets get further apart at Γ. As $\alpha \to \pi$ the separation between the sheets at Γ approaches a full lattice constant c and the contribution to $\theta_{z\Omega}$ approaches π. This expectation is confirmed in Fig. 3, where we plot the evolution of θ *vs.* α, and also its two individual contributions $\theta_{z\Omega}$ and $\theta_{\Delta xy}$, as computed from Eqs. (13-14). Compared to $\theta_{z\Omega}$, the non-topological $\theta_{\Delta xy}$ term is almost negligible everywhere around the adiabatic loop, with the possible exception of the vicinity of the Z_2-odd phase where it reverses suddenly, as a result of the WCC sheets from adjacent layers coming close to each other at the Γ-point.

As α passes through π there is a Dirac touching at Γ between sheet 2 in the home cell and sheet 1 in the cell above, with a hand-off of -2π units of Berry curvature (or a Chern number of -1) from the former to the latter, and with the concentration of Berry curvature near Γ in band 2 switching from $-\pi$ to π. A direct evaluation of Eq. (13) would show $\theta_{z\Omega}$ and θ dropping discontinuously by 2π as α crosses through π, but we make use of the gauge freedom to apply a 2π shift of θ to impose physical continuity when drawing the curves in Fig. 3.

Of course, here we have illustrated the behavior of just one model system, and we have found that the pumping of θ by 2π is accomplished by a series of touching events between WCC sheets, such that one Chern number of Berry curvature is handed off to the neighboring sheet with each touching. But having seen this, it is now clear in retrospect that *any cycle that pumps θ by 2π must involve such a sequence of touching events.* For, if these events did not occur, the CSA coupling could not be passed along by a lattice vector during the cycle. Incidentally, this observation also explains why a non-trivial θ pumping cycle is impossible in a system with a single occupied band, since in this case the WCC sheets are always separated by $c\hat{z}$ and can never touch.

One can also consider the corresponding evolution of the Berry curvatures and Chern transfers for finite slabs, where the bulk of the slab undergoes the same cyclic evolution. If the surface Hamiltonian could be constantly readjusted so as to remain insulating, the net result at the end of the cycle would be to change the surface AHC by $\pm e^2/h$ at the bottom and top surfaces of the slab respectively. In the more common case that the surface returns to its initial state at the end of the cycle, the AHC must return to itself too, so the slab is topologi-

cally required to have a metallic surface phase over some interval of α, such that the extra Chern number can be removed. The existence of such surface states can be an experimental signature characterizing any adiabatic loop with non-zero second Chern number.

In summary, we have demonstrated that an analysis of the WCC sheets as defined in the HWF representation, which had previously been shown to be useful for identifying and visualizing the topological properties of non-trivial insulating phases, also provides an insightful characterization of a non-trivial parametric loop characterized by a second Chern number. By defining Berry connections and curvatures associated with the WCC sheets, we have derived a new formula for the CSA axion coupling θ, emphasizing that it is naturally decomposed into a topological Berry curvature dipole term and a non-topological correction term. We showed that the WCCs exhibit a non-trivial zigzag behavior as a function of the loop parameter. However, unlike for a Chern or Z_2-odd insulator, this zigzag evolution of the WCCs describes not the pumping of charge, but the pumping of layer Berry curvature defined in terms of the HWFs. In our formulation the 2π ambiguity of θ is readily evident when some sheets have non-zero Chern numbers, in which case a different assignment of sheets to the home unit cell can shift θ by 2π, and the link to the surface anomalous Hall conductivity becomes more direct. We also speculate that Eqs. (13-14) may provide a more efficient practical means of computing θ than those used previously, since there is no need to establish a smooth gauge in the 3D Brillouin zone. In any case, we believe that our extended development of the HWF representation should prove broadly useful in characterizing the adiabatic evolution of topological materials and their magnetoelectric properties.

This work was supported by NSF Grant DMR-14-08838, and was inspired in part by preliminary calculations of Sinisa Coh. We thank Ivo Souza for useful discussions.

* Electronic address: mtaheri@physics.rutgers.edu

[1] A. M. Essin, J. E. Moore, and D. Vanderbilt, Phys. Rev. L. **102**, 146805 (2009).
[2] X.-L. Qi, T. L. Hughes, and S.-C. Zhang, Phys. Rev. B **78**, 195424 (2008).
[3] M. Taherinejad, K. F. Garrity, and D. Vanderbilt, Phys. Rev. B **89**, 115102 (2014).
[4] A. A. Soluyanov and D. Vanderbilt, Phys. Rev. B **83**, 235401 (2011).
[5] A. Alexandradinata, B. Andrei Bernevig, arXiv:1208.4234 (2012).
[6] A. Alexandradinata and B. Andrei Bernevig, arXiv:1409.3236v1 (2014).
[7] C. Sgiarovello, M. Peressi, and R. Resta, Phys. Rev. B **64**, 115202 (2001).
[8] N. Marzari and D. Vanderbilt, Phys. Rev. B **56**, 12847 (1997).
[9] X. Wu, O. Diéguez, K. M. Rabe, and D. Vanderbilt, Phys. Rev. L. **97**, 107602 (2006).
[10] R. Yu, X. L. Qi, A. Bernevig, Z. Fang, and X. Dai, Phys. Rev. B **84**, 075119 (2011).
[11] D. J. Thouless, Phys. Rev. B **27**, 6083 (1983).
[12] L. Fu, C. L. Kane, and E. J. Mele, Phys. Rev. Lett. **98**, 106803 (2007).